Virtual Dike: multiscale simulation of dike stability

Melnikova, N.B.; Shirshov, G.S.; Krzhizhanovskaya, V.V.

DOI
10.1016/j.procs.2011.04.084
Publication date
2011
Document Version
Final published version
Published in
Procedia Computer Science

Available online at www.sciencedirect.com

ScienceDirect

Procedia Computer Science 4 (2011) 791–800

Procedia Computer Science

International Conference on Computational Science, ICCS 2011

Virtual Dike: multiscale simulation of dike stability

N.B. Melnikova[c,a,b], G.S. Shirshov[a,b], V.V. Krzhizhanovskaya[a,b,c]*

[a] *University of Amsterdam, The Netherlands*
[b] *St. Petersburg State Polytechnic University, Russia*
[c] *National Research University ITMO, Russia*

Abstract

We present a Virtual Dike simulation module developed as a part of a flood Early Warning System (EWS) for the *UrbanFlood* project. The *UrbanFlood* EWS is a distributed system that analyzes sensor data received in real-time from flood defenses (dikes, dams, etc.) and simulates dike stability, breaching and flood propagation. The aim of the Virtual Dike module is to develop an advanced multiscale multiphysics simulation laboratory for expert users and numerical model developers. This lab is used to validate simulation models, to plan experiments and to investigate physical processes influencing dike stability and failure. In the first stage of the project, we have studied the structural stability of the Live Dike, a dike protecting a seaport in Groningen, the Netherlands. The four cross-sections of the dike are equipped with sensors of pore pressure and inclination. For each section, 2D simulations of flow through porous media and dike deformations have been performed under tidal water load. Simulation results have been compared with the sensors data in order to calibrate soil properties. Pore pressure, stress dynamics and structural stability of the dike have been analyzed.

Keywords: Virtual Dike; flow; porous media; structural dynamics; flood protection; early warning system; UrbanFlood.

1. Introduction

Recent catastrophic floods around the world have spawn a large number of projects aimed at the development of stronger and "smarter" flood protection systems. The FP7 project SSG4Env is focused on development of semantic sensor grids for environment. Flood Probe (also funded by FP7) coordinates work on combination of sensor measurement techniques. Flood Control 2015 is aiming to share sensor measurements datasets and provide a user interface to explore sensor data for researchers, technical maintainers and civil population. The IJkdijk project [1] is a unique experimental series to investigate dike failure mechanisms. The tests are carried out on full-scale experimental dikes equipped with large sets of sensors. The project has produced extremely detailed and precious datasets of sensor data, including pore pressure, inclination and temperature measurements. The project data are available to the scientific community and can serve for gaining better knowledge and understanding of dike failure mechanisms.

The *UrbanFlood* EC FP7 project [2,3,4] is the first endeavor that unites the work on all the aspects studied in the

* Corresponding author. *E-mail address*: V.Krzhizhanovskaya@uva.nl

 Selection and/or peer-review under responsibility of Prof. Mitsuhisa Sato and Prof. Satoshi Matsuoka
doi:10.1016/j.procs.2011.04.084

projects mentioned above. One of the key challenges is the development of computational models. Here we describe a Virtual Dike module for analyzing dike stability and predicting risk of dike failure.

The Virtual Dike is being developed as an advanced multiscale multiphysics simulation lab for expert users and model developers. This virtual lab is used for validation of all the models involved in the modeling cascade, and serves as a research field for experiment planning and understanding the underlying physical processes influencing dike stability and failure. Comparison of simulation results with the experimental data allows determining the material properties and computational model parameters that best represent real-life dikes, with all their inhomogeneities and special features.

Structural analysis of dike stability includes analyzing several possible failure mechanisms, different in their physical nature and acting on different scales. These mechanisms are slope instability, surface erosion and piping. Surface erosion and piping are caused by particles washed out of the soil by water; they act on microscopic scale. Engineering criteria used nowadays to predict these phenomena are obtained using macroscopic description of these mechanisms with some heuristic corrections [17]. A detailed study would require fluid flow modeling coupled with particle dynamics modeling. Slope instability can be characterized as macroscopic physical process: failure happens when sliding between planes of the material occurs. In this case soil can be considered as continuous media with elastic or elasto-plastic constitutive behavior [7,16]. The problem requires modeling of flow through porous media and solving structural task to analyze dike stability. Pore pressure, acting inside of the material as volume load, is transferred to the structural part of analysis and affects stresses and deformations in the soil, usually unloading the construction (the effect was first observed by K. Terzaghi [5]). Backward influence of pores expansion, giving additional source terms in porous flow equation, makes a task highly non-linear, fully coupled fluid-structure interaction problem. M.A. Biot [6] was one of the first researchers to investigate this, using Darcy's equation for porous flow and linear elastic theory in structural analysis. Biot poroelasticity theory is widely used for modeling macroscopic behavior of soils with porous flow [6]. If a dike is subjected to a dynamic tidal load, the phreatic surface (a border between saturated and unsaturated zones in soil) changes its location and shape dynamically. This effect can be taken into consideration either by solving Darcy's equation in saturated zone using finite element (FE) method with deforming mesh [10] or using special computational techniques with a fixed FE mesh (built for the whole soil domain), finding unsaturated cells and excluding their contribution to the system of FE flow equations [9]. Another way to solve this problem is to use Richards equation, modeling wetting and drying of the soil. This allows to get phreatic surface shape automatically and moreover, to take into consideration raining condition. In the present work, we use Richards equation with the Van Genuchten model [8] for porous flow in unsaturated zone, coupled with linear elastic structural equations.

2. A test case: sea dike in Eemshaven

LiveDike is protecting a seaport in Groningen, see Figure 1a. This dike has been equipped with sensors, and data stream is available in real-time via a LiveDike Dashboard [11].

Figure 1. (a) Location of the LiveDike (Eemshaven) in Google Maps; (b) LiveDike with marked sensor locations

Sensor GPS locations are shown in Figure 1b. Sensors are placed in four dike cross-sections, see Figure 2a. These cross-sections have been simulated in 2D models under tidal water loading. Simulation results have been compared with the pore pressure sensors data in order to calibrate model parameters, so that virtual and real sensor values agree.

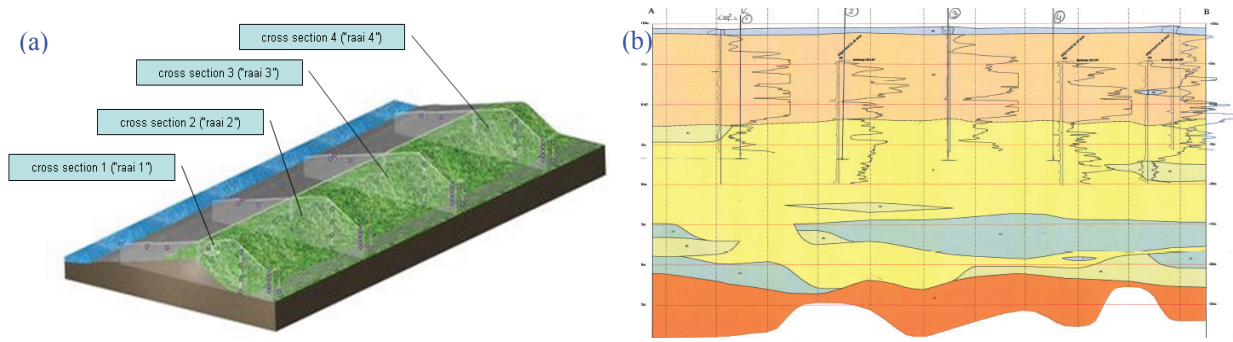

Figure 2. (a) LiveDike geometry scheme and cross-sections where the sensors are located; (b) LiveDike soil build-up in the in the central longitudinal cross-section

LiveDike internal structure is well documented. *UrbanFlood* community has been granted access to the data on soil build-up shown in Figure 2b. The dike consists mainly of building sand (light orange color) with a 60 cm layer of clay on top (light blue stripe). Below the dike lies a coarse sand (yellow area), with some smaller zones of sand mixed with clay layers (light green). Besides that, there are clay zones lying below the depth of 15 m (light blue) and Pleistocene sand below the depth of 20 m (bright orange), but these deep areas were not included into a simulation domain for the present simulation (see Section 3.2).

3. Virtual Dike modeling approach

3.1. Governing equations

The problem requires modelling of coupled fluid-structure interaction, with non-linear dike material properties. The fluid sub-model describes the dynamics of flow through porous soil, with the pressure-based form of Richards equation [14,15] for wetting and drying of the area above phreatic surface. The Van Genuchten model [8] is used to describe the properties of unsaturated soil. The pore volume expands with the expansion of the media, therefore water content increases. This process is modeled with additional source term in the right hand side of the Richards equation:

$$(C+\theta_e S)\frac{\partial p}{\partial t}+\nabla\cdot[-\frac{K_S}{\mu}k_r\nabla(p+\rho g z)]=\frac{\partial \varepsilon}{\partial t}, \tag{1}$$

where $\varepsilon=\varepsilon_x+\varepsilon_y$ is coefficient of volume expansion of porous media, obtained form structural equations (2); p is pressure, [Pa]; $C=C(p)$ is specific moisture capacity [1/Pa], $C=\partial\theta/\partial p$; $\theta_e=\theta_e(p)$ is effective water content; S is a storage coefficient, [1/Pa]; t is time, [s]; K_S is permeability of saturated media, [m^2]; $k_r=k_r(h)$ is relative permeability, computed using Van Genuchten formulas [8]; μ is dynamic viscosity of water, [Pa·s]; g is standard gravity, [m/s^2]; ρ is water density [kg/m^3]; z stands for coordinate of vertical elevation, [m].

The structural sub-model describes deformation dynamics of the dike under tidal pressure load, gravity and volumetric pore pressure p load obtained from flow simulation. Linear elastic constitutive behavior is used for describing sand and clay properties:

$$\begin{cases}\nabla\cdot\underline{\underline{\sigma}}-\nabla p+\rho_s\underline{g}=0\\ \underline{\underline{\sigma}}=\lambda\varepsilon\underline{\underline{E}}+2\mu\underline{\underline{\varepsilon}}\end{cases}, \tag{2}$$

where $\underline{\underline{\sigma}}=\sigma_{ij}\underline{e}_i\underline{e}_j,\ i,j=1,2$ is effective stress tensor [Pa] with component matrix $\sigma_{ij}=\begin{bmatrix}\sigma_x & \tau_{xy}\\ \tau_{xy} & \sigma_y\end{bmatrix}$;

$\underline{\underline{\varepsilon}} = \varepsilon_{ij} \underline{e}_i \underline{e}_j$, $i, j = 1,2$ is deformation tensor having component matrix $\varepsilon_{ij} = \begin{bmatrix} \varepsilon_x & \gamma_{xy} \\ \gamma_{xy} & \varepsilon_y \end{bmatrix}$; $\underline{e}_i, i = 1,2$ are vectors of coordinate basis; λ, μ are Lame parameters, [Pa]; $\underline{g}$ is gravity vector, ρ_s is soil density, [kg/m^3]; ∇ is Laplace differential operator.

Dike stability is evaluated by Mohr-Coulomb failure criterion for materials with no cohesion [7], which shows that failure occurs when shear stress acting on some plane reaches the limit of material resistance provided by an internal friction mechanism. The condition of dike stability is then as follows:

$\tau_m \le \sigma_m \tan\phi$ for all material points in the simulation domain,

where ϕ is friction angle [grad], τ_m is maximal shear stress in the point, [Pa]; σ_f is corresponding normal stress in the point, [Pa].

Bishop criterion, which is widely used in engineering practice to detect a slope stability margin, employs Mohr-Coulomb criterion as a basis with an additional assumption that the slip surface is circular [7].

In terms of principal stresses, Mohr-Coulomb criterion can be written as

$stab \ge 0$, where $stab = \frac{\sigma_1 - \sigma_3}{2} - \frac{\sigma_1 + \sigma_3}{2} \tan\phi$,

where σ_1 is maximal principal stress, σ_3 is minimal principal stress. The value of *stab*=0 indicates the onset of local instability; *stab* < 0 denotes an unstable condition; and *stab* > 0 predicts stability. Negative values of *stab* in a relatively large continuous zone predict dike failure.

3.2. Computational domain and meshing

We consider a two-dimensional planar model of the LiveDike transversal cross-section. The dike itself is 9 meter high and about 60 meter wide. We have added into a simulation domain a fragment of sea floor below the dike, which is 120 m wide and 20 m deep. The simulation domain is shown in Figure 3a. The domain includes three homogeneous zones: clay (red layer on top of the dike), sand1 (blue area in the middle) and sand2 (grey zone in the bottom). This is a simplified model of the real soil distribution, adopted for the initial tests. The model only includes vertical inhomogeneity. Later it will be shown that horizontal inhomogeneity should also be considered in order to obtain a good agreement between simulation results and sensor data (see Section 4).

The finite element mesh (Figure 3b) was built in Comsol software package [12]. It consists of triangular finite elements of second order. Refinement zone is located around phreatic line, where flow parameter gradients can be high and dynamically changing. The total number of elements is about 15000.

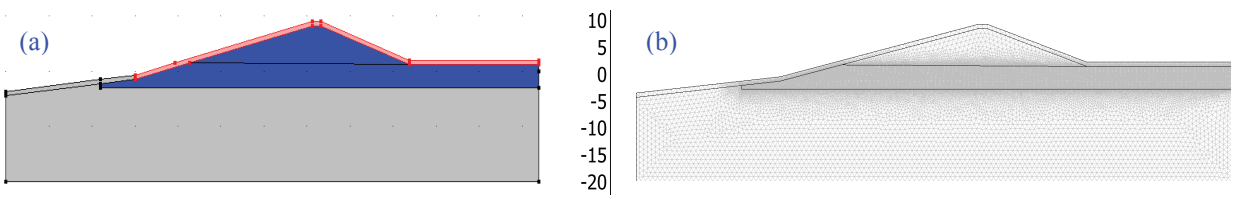

Figure 3. (a) Simulation domain (b) Finite element mesh with refinement area near the phreatic line

3.3. Boundary conditions

The sensor data from sea water level is employed in the model via harmonic approximation of the signal, which is applied as a boundary condition (see Figure 4).

Boundary condition zones are presented in Figure 5. Boundary conditions for the **structural sub-model** are:

At the **seaside** (green line in Figure 5a) pressure is calculated as

$$p = \rho g[h_{amp} \cdot \sin(\omega(t - t_0)) - y], \quad (3)$$

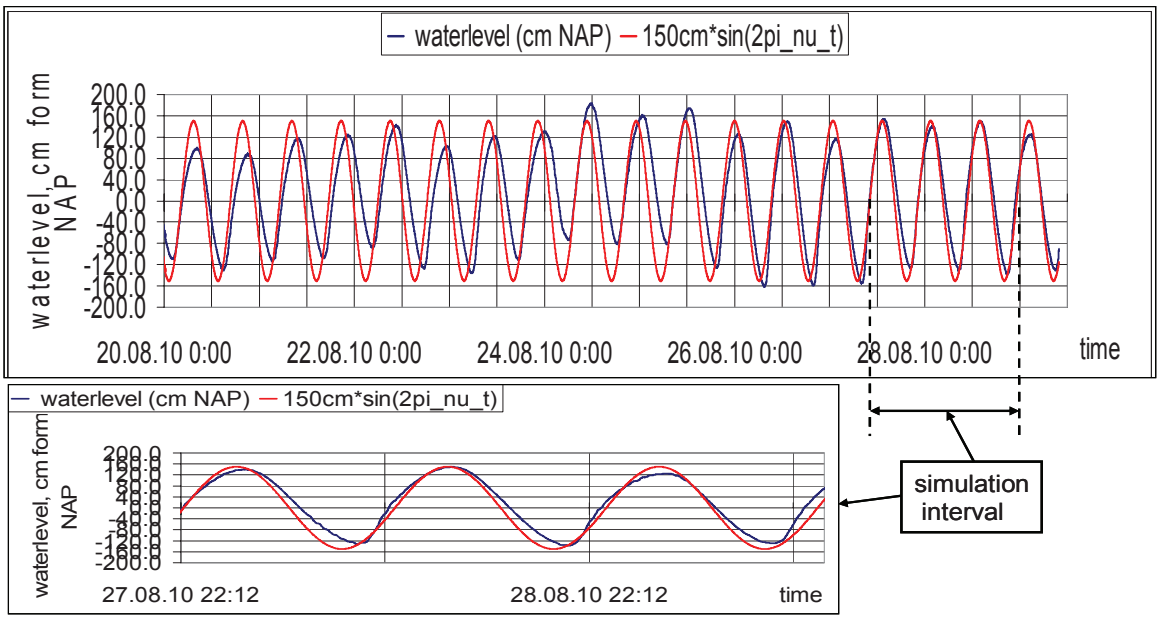

Figure 4. Water level dynamics obtained from sensor data and harmonic approximation

where h_{amp} = 1.5 *m* is the amplitude of tidal oscillation of sea water level; $\omega = 2\pi / T$ is radial frequency of the tidal cycle, and tidal period T = 12 hrs 25 min; y [m] is a vertical coordinate relative to the reference water level.

At the **vertical borders** (red lines in Figure 5a), a symmetry condition is imposed (displacements normal to boundary are zero). The **base** of the body is fixed (blue line). Remaining borders are free (black lines).

Boundary conditions for the **flow sub-model** are the following:

At the **inlet** (black line in Figure 5b) pressure is calculated as

$$p = \rho g[h_{amp} \cdot \sin(\omega(t - t_0)) - y]. \quad (4)$$

At the **outlet** (cyan line in Figure 5b) water level stays at the Dutch water reference level (common abbreviation for the reference level in Dutch is NAP), therefore pressure can be defined as

$$p = -\rho g y. \quad (5)$$

Zero flux boundary condition is imposed on the remaining boundaries (magenta lines in Figure 5b).

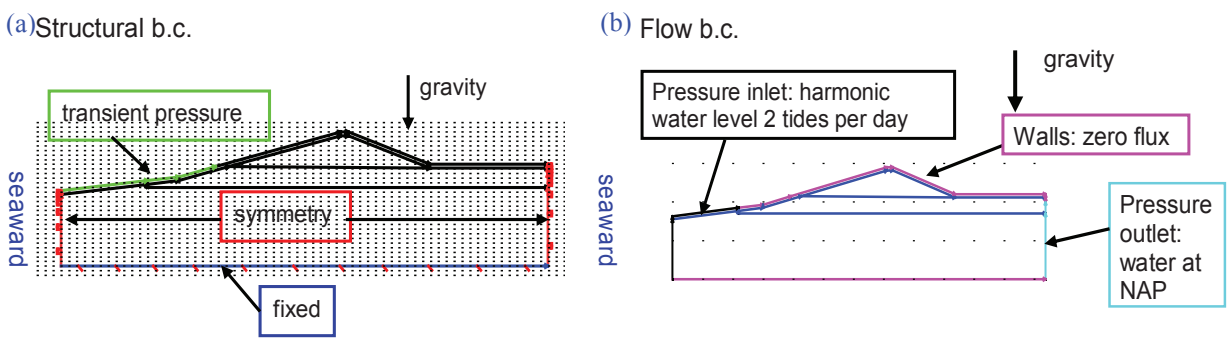

Figure 5. Boundary conditions: (a) for the structural sub-model; (b) for the fluid sub-model

3.4. Initial conditions

In order to begin transient simulations, we need to obtain initial pressure and saturation distribution in the dike. For that purpose additional transient simulation with stationary boundary conditions has been performed. Boundary conditions at the inlet and at the outlet are set $p = -\rho g y$ (water level is at the NAP, Netherlands reference sea level). This simulation starts form an arbitrary pressure distribution (constant, uniform) and converges to the steady-state pressure distribution used in the transient simulations as initial condition.

3.5. Implementation

Partial differential equations (1), (2) with the boundary conditions (3-5) are solved by the finite element method: the computational domain is discretized into small elements; and original equations are reduced to a system of ordinary differential equations solved by an implicit time integration scheme. Simulations have been performed in the finite element software package Comsol [13].

The equations are non-linear due to the non-linear constitutive behavior of the soil and fluid-structure coupling phenomenon. Iterative Newton-Raphson method has been used to linearize differential equations at each integration step. Direct parallel UMFPACK and PARDISO solvers have been used for solving the system of linear algebraic equations within each iteration.

Porous flow simulations typically require up to 2 GB of RAM. Each simulation took about 2 hours to perform on two processors of a laptop AMD Athlon Dual-Core 1.9 GHz, 2 GB of RAM, under Windows operating system. Coupled fluid-structure problem requires up to 8 GB of memory and 6-10 hours to perform on Intel Xeon Dual Core PC 3 Hz, 8 GB of RAM. The solver has been ported to SARA [18] Clouds to run time-consuming coupled simulations.

SARA HPC cloud system is hosted on a 128-core cluster equipped with the dual quad-core 2.2 GHz CPUs. SARA employs OpenNebula open source cloud computing management toolkit with KVM as the Virtual machine software. Clouds are customized for the specific simulation. The number or cores (from 1 to 8) and the amount of RAM (up to 24 GB) are set according to the required calculation time. Clouds have 500 GB local hard disk space with the 100 TB backup storage. Aggregated connection speed from the cluster to storage is 20 Gb/s. Clouds are also provided with the high-speed 1 Gb/s network.

4. Parallel efficiency benchmarking

Parallel efficiency of the UMFPACK and PARDISO solvers has been tested on SARA Clouds in shared memory mode on 2, 4, 6 and 8 computational cores. Number of degrees of freedom varied from 60 000 to 250 000, which corresponds to small and medium model size. The value of parallel efficiency varied from almost ideal 98 % (for 2 cores, 250 000 unknowns) to 15 % (for 8 cores, 60 000 unknowns). Overall tendency has proved that the efficiency is highest when we use a small number of cores and a large number of unknowns (see Figure 6). A more detailed description of the parallel tests is given in [12]. Low parallel efficiency (less then 50%) has been observed for number of cores 6 and 8. The reason may lie in high process synchronization costs, but this issue should be investigated with a parallel profiler.

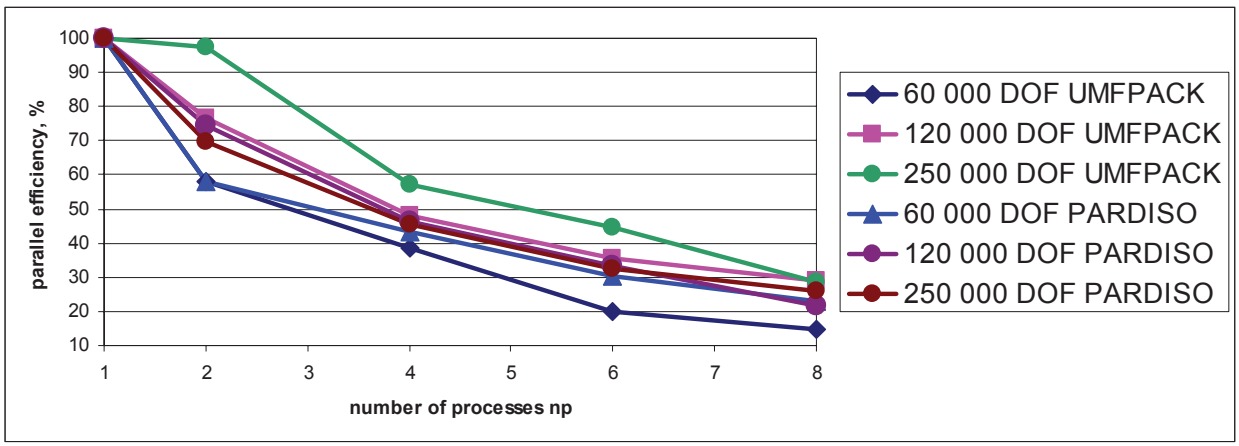

Figure 6. Parallel efficiency for UMFPACK and PARDISO solvers

5. Simulation results

Pore pressure fields are shown in Figure 7 for the high and low tides. The unsaturated zone is shown with the white color, so that the phreatic line is depicted as a boundary between saturated and unsaturated zones.

During the high tide, water level is higher at the sea side (left boundary). At the right-hand side, phreatic surface is fixed due to the impose boundary condition – stationary water level. As we recently found, at the meeting with the dike manager, recently a channel corresponding with the sea has been dug along the dike at the landside and therefore the right-hand side boundary condition shall be corrected. As animations showed, the phreatic line is moving like a wave (with one end fixed), due to the harmonic dynamics of the tidal water load.

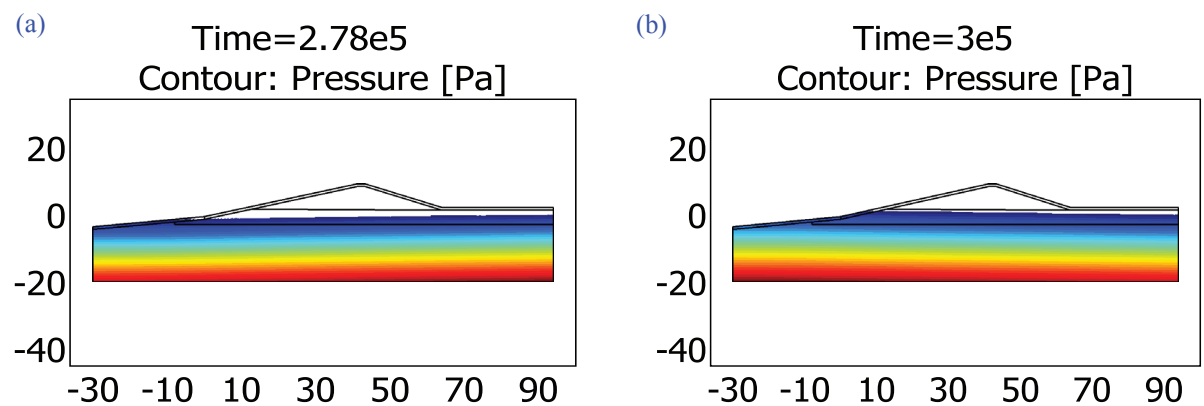

Figure 7 . Pore pressure field: (A) – low tide; (B) – high tide

Fragments of the effective saturation field at the seaside are shown in Figure 8 for the high and low tides.

During the low tide, water level inside the dike decreases and the sand located above the water table gets dry (yellow color in Figure 8a). During the low tide the upper layer of clay, located above the water table, stays wet due to high water capacity of clay. In the high tide phase, water table rises and that can be seen in Figure 8b (blue saturated zone has enlarged, relatively to the Figure 8a).

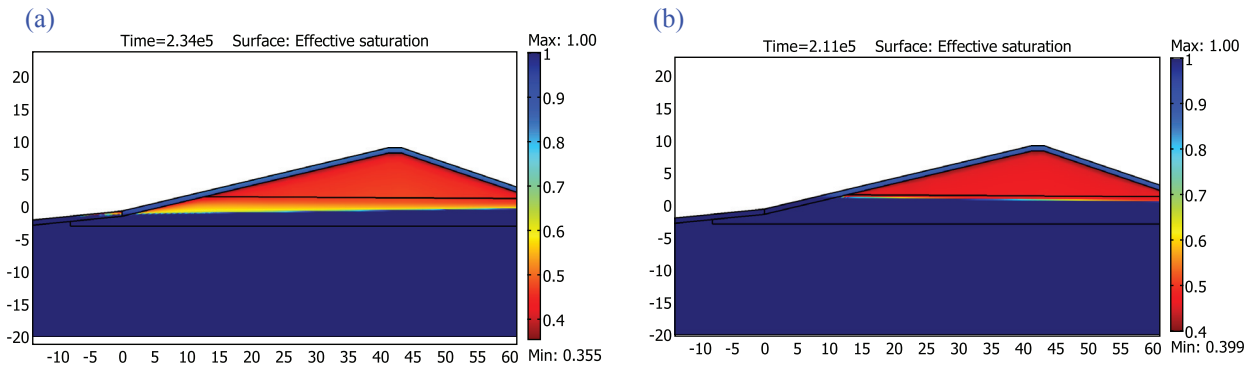

Figure 8. Effective saturation field: (a) – low tide; (b) – high tide

Structural displacements field in one moment of time is shown in Figure 9a. The displacements are composed of: a) static soil settlement under gravity load (maximal at the top of the dike) and b) transient displacements resulting from tidal pressure at the seaside and volume pore pressure load. Total displacements are maximal at the top of the dike due to gravity settlement component. The field of stability parameter *stab* in one moment of time is shown in Figure 9b. At tidal load *stab* is positive and the dike is stable.

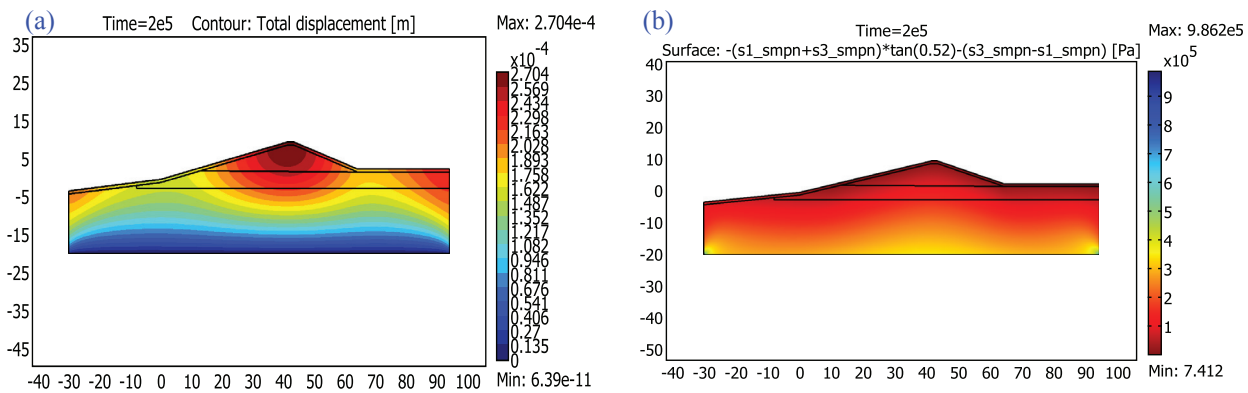

Figure 9. (a) Structural displacements field; (b) Value of stability parameter *stab*. *stab* > 0 predicts dike stability.

We have considered two different values of saturated permeability K_S for coarse sand, located in the deep part of the dike (gray zone in Figure 3a): $K_S = 10^{-9}$ m^2 and $K_S = 10^{-10}$ m^2. In each case, a comparison of numerical results with real sensor data has been performed for pore pressure dynamics. The comparison has been made in the points of sensor locations. For the Livedike, in each section we have 3 sensors located in saturated zone and providing informative pore pressure data (they are shown in Figure 10 within green circle). A comparison has been made for all the points, in four sections of the dike. The results are shown in Figure 10 for the section #1, for two sensors. Real sensor signals are shown with bold lines (green – sensor "E4", blue – sensor "G2"). "Virtual" sensor signals (obtained from simulation) are shown with thin lines. For sensor "E4" (left plot), located in the coarse sand zone, the agreement is quite good for value of $K_S = 10^{-9}$ m^2. Sensor "G2" is located in the same zone as "E4", but real sensor shows that the amplitude of pore pressure oscillations is much lower for "G2" than for "E4". The reason for this difference is in local inhomogeneities of the soil, which must be taken into consideration in further simulations. Comparison of the data for sensor "G2" shows that the real sensor is placed in a less permeable zone than the zone of the virtual sensor is. In virtual model, permeability values will be corrected and G2 sensors will be surrounded with less permeable soil.

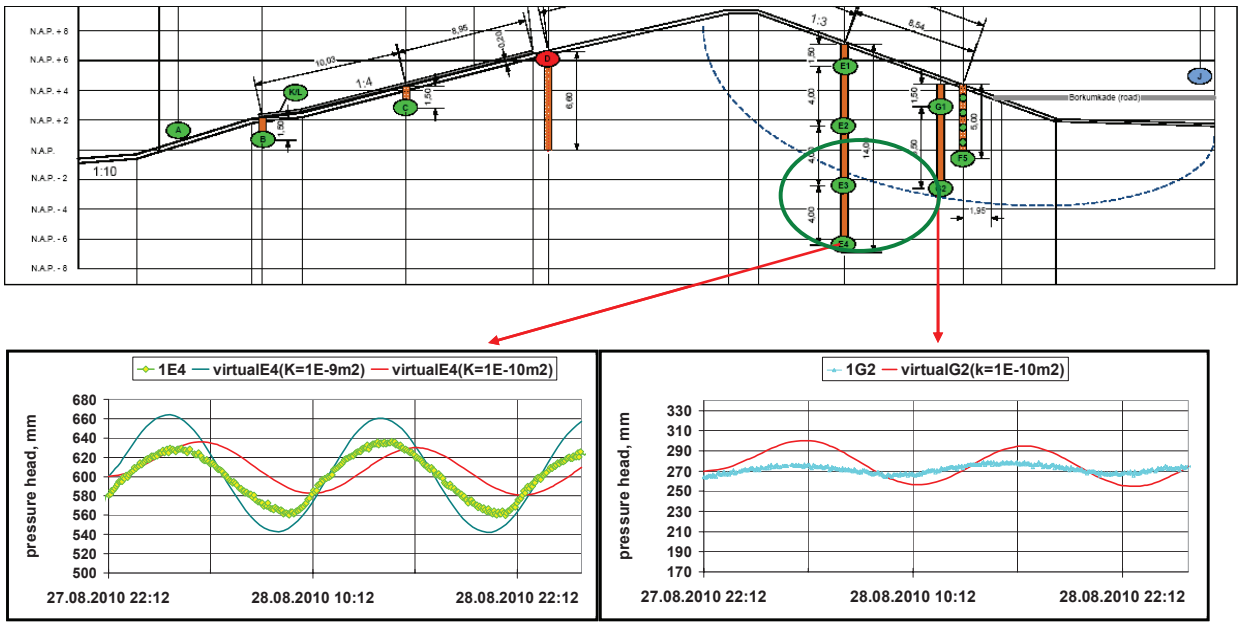

Figure 10. Pressure head dynamics obtained from real and "virtual" pore water pressure sensors 1E4 and 1G2, installed in the first cross-section of the dike

6. Conclusions and plans

Pore pressure and stress dynamics in the dike have been obtained in the present work, under tidal load. Comparison of real and virtual pore pressure sensor data shows that local inhomogeneities should be included into the model to properly simulate real water pressure dynamics. Parallel efficiency of the Comsol UMFPACK and PARDISO solvers has been tested, in shared memory mode. Low parallel efficiency (less then 50%), possibly caused by high process synchronization costs, has been observed for number of cores 6 and 8.

For the LiveDike porous flow modelling, we plan to implement a more detailed heterogeneous soil model in order to obtain a better agreement between the pore pressure fields from real sensors and from simulations. Flood condition is to be investigated, including porous flow modelling and dike slope stability analysis. Simulations will be performed on the SARA Clouds. Next, we will model dike failure mechanisms based on the IJkdijk experiments, including slope instability, piping and surface erosion. In addition, we plan to explore the system identification theory approach to build simplified models based on the sensor data analysis and advanced modelling. Finally, the Virtual Dike will be integrated into the Common Information Space to receive sensor input automatically and to produce real-time simulation results for displaying them on a multi-touch table or a web-based decision support system.

Acknowledgements

This work is supported by the EU FP7 project *UrbanFlood*, grant N 248767, and the *Leading Scientist Program* of the Government of the Russian Federation, contract 11.G34.31.0019. The work is carried out in close collaboration with a number of organizations and individuals (listed in alphabetical order): AlertSolutions, particularly Erik Peters; BiG Grid, advanced ICT research infrastructure for e-Science; Deltares, particularly Andre Koelewijn; IJkDijk Association; Rijkswaterstaat, Ministerie van Verkeer en Waterstaat; SARA Computing and Networking Services, particularly Tom Visser and Floris Sluiter; UvA IBED-CGE, particularly Lourens Veen; UvA GIS, particularly Studio Guido van Reenen; WaterNet, particularly Rob van Putten; Waterschap Noorderzijlvest, particularly Christiaan Jacobs.

References

1. IJkdijk project http://www.ijkdijk.eu/
2. V.V. Krzhizhanovskaya at al. Flood early warning system: design, implementation and computational modules. Proceedings of the International Conference on Computational Science, ICCS 2011. Procedia Computer Science 00(2011) 000–000 (In print)
3. *UrbanFlood* EU FP7 project http://www.urbanflood.eu
4. V.V. Krzhizhanovskaya. A roadmap to multiscale modeling of flood defense systems: from sand grain to dike failure and inundation. Proceedings of ASME 2010 Computers and Information in Engineering Conference IDETC/CIE 2010, Montreal, Canada. Paper # DETC2010-28967
5. K. Terzaghi, Theoretical Soil Mechanics, Wiley, 1943.
6. M.A. Biot, "Theory of elasticity and consolidation for a porous anisotropic solid," J. Appl. Phys., vol. 26, no. 182, 1955..
7. A. Verruijt. Soil Mechanics. Delft University of Technology, 2001. 315 pages.
8. M.T. van Genuchten. A closed form equation for predicting the hydraulic conductivity of unsaturated soils. Soil Science Society of America Journal 44: 892-898.
9. A. Larabi, F. De Smedt. Numerical solution of 3-D groundwater flow involving free boundaries by a fixed finite element method. Journal of Hydrology 201 (1997) 161-182. Elsevier.
10. P. Knupp. A moving mesh algorithm for 3-D regional groundwater flow with water table and seepage face. Advances in Water Resources. Volume 19, Issue 2, 1996, Pages 83-95
11. Livedike dashboard http://livedijk-www.ict.tno.nl/
12. N.B. Melnikova, G.S. Shirshov ,V.V. Krzhizhanovskaya, N.N. Shabrov. Virtual Dike and Flood Simulator: Parallel distributed computing for flood early warning systems. Proceedings of the 5th International Conference on Parallel Computating Technologies PAVT-2011, 28 March – 1 April 2011, Moscow, Russia. pp. 1-9 (In print)
13. Official site of COMSOL software http://www.comsol.com
14. J. Bear. Dynamics of Fluids in Porous Media, Elsevier Scientific Publishing Co, 1972.
15. J. Bear. Hydraulics of Groundwater, McGraw-Hill, 1979.
16. A.R. Koelewijn, M.A.Van. Monitoring of the test on the dike at Bergambacht: design and practice. Proceedings of XIII ECSMGE 2003, Prague, Czech Republic.
17. W. Allsop, A. Kortenhaus, M. Morris. Failure Mechanisms for Flood Defence Structures. FLOODsite Report. T04_06_01. 2007 http://hikm.ihe.nl/floodsite/data/Task4/pdf/failmechs.pdf
18. SARA Computing and Networking Services, http://www.sara.nl/